NIH Public Access
Author Manuscript
Dev Cell. Author manuscript; available in PMC 2014 January 14.

Published in final edited form as:
Dev Cell. 2013 January 14; 24(1): . doi:10.1016/j.devcel.2012.11.010.

Repeated, long-term cycling of putative stem cells between niches in a basal chordate

Yuval Rinkevich[1,2,*,§], **Ayelet Voskoboynik**[2,*,§], **Amalia Rosner**[1], **Claudette Rabinowitz**[1], **Guy Paz**[1], **Matan Oren**[1], **Jacob Douek**[1], **Gilad Alfassi**[1], **Elizabeth Moiseeva**[1], **Katherine J Ishizuka**[2], **Karla J Palmeri**[2], **Irving L. Weissman**[2], and **Buki Rinkevich**[1,§]

[1]Israel Oceanographic and Limnological Research, National Institute of Oceanography, PO Box 8030, Tel Shikmona, Haifa 31080, Israel

[2]Institute of Stem Cell Biology and Regenerative Medicine, Departments of Pathology and Developmental Biology, Stanford University School of Medicine, Stanford, CA 94305, USA, and Hopkins Marine Station, Pacific Grove, CA 93950 USA

Summary

The mechanisms that sustain stem cells are fundamental to the maintenance of tissues/organs. Here we identify 'cell-islands' (CIs) as a niche for putative germ and somatic stem cells in *Botryllus schlosseri*, a colonial chordate that undergoes weekly cycles of death and regeneration. Cells within CIs express markers associated with germ and somatic stem cells and gene products that implicate CIs as signaling centers for stem cells. Transplantation of CIs induced long-term germ-line and somatic chimerism, demonstrating self-renewal and pluripotency of CI-cells. Cell labeling and *in-vivo* time-lapse imaging of CI-cells reveal waves of migrations from degrading CIs, into developing buds, contributing to soma and germ-line development. Knockdown of *cadherin*, which is highly expressed within CIs, elicited the migration of CI-cells to circulation. *Piwi*-knockdown resulted in regeneration arrest. We suggest that repeated trafficking of stem cells allow them to escape the constraints imposed by the niche, thereby promoting their self-preservation throughout life.

Keywords

ascidian; *Botryllus schlosseri*; *cadherin*; development; endostyle; germline; migration; niche; stem cells

Introduction

Botryllid ascidians (e.g., *Botryllus schlosseri, Botrylloides leachi*) are colonial marine protochordate organisms that are composed of up to several thousands of genetically identical individuals, called zooids (Fig. 1, A, B). Each zooid is 2-3mm long and is embedded within the tunic, a semi-translucent gelatinous matrix. Groups of zooids are arranged in systems connected to each other through a delicate one cell thick vasculature of

© 2012 Elsevier Inc. All rights reserved.

[§]Corresponding authors: Buki Rinkevich, Tel: +972 4 8565273, Fax: +972 4 8511911, buki@ocean.org.il, Yuval Rinkevich, Tel: 650 7236520, Fax: 650 7234034, ryuval@stanford.edu, Ayelet Voskoboynik, Tel: 831 6556244, Fax: 650 7234034, ayeletv@stanford.edu.
[*]These authors contributed equally

Publisher's Disclaimer: This is a PDF file of an unedited manuscript that has been accepted for publication. As a service to our customers we are providing this early version of the manuscript. The manuscript will undergo copyediting, typesetting, and review of the resulting proof before it is published in its final citable form. Please note that during the production process errors may be discovered which could affect the content, and all legal disclaimers that apply to the journal pertain.

NIH-PA Author Manuscript
NIH-PA Author Manuscript
NIH-PA Author Manuscript

NIH-PA Author Manuscript

NIH-PA Author Manuscript

NIH-PA Author Manuscript

extra-corporeal blood vessels, which terminate in ampullae- pear-shaped extensions which fringe the colony (Fig. 1, A, B).

Once the planktonic tadpole-like larvae has settled and metamorphosed into the first founder zooid, a colony grows through weekly and synchronized cycles of asexual stages of development, called blastogenesis (Manni et al., 2007). Blastogenesis occurs in four major stages (A-D), during which new buds (1-3) emerge from the body wall of each parental zooid (Fig. 1C). In a few days, the simple bud, through several stages of evagination and invagination of complex cellular assemblies forms organs as distinct and diverse as a two chambered heart, gill slit, a complete gastrointestinal system, a neural network, 10 morphological different blood cell types, etc. Each blastogenic cycle ends in a massive apoptotic and phagocytic event of all parental zooids, concurrent with rapid development of primary buds to the adult zooid stage (blastogenic stage D, also called ‘takeover’; Lauzon et al., 1992).

Several observations indicate that colonial Botryllid ascidians harbor germ and somatic stem cells that propagate throughout the life of the animal. Botryllid ascidians can regenerate whole organisms equipped with a reproductive system from experimentally separated blood vessels (Oka and Watanabe, 1957, 1959, Sabbadin et al., 1975, Rinkevich et al., 1995, Voskoboynik et al., 2007, Brown et al., 2009), a process termed ‘Whole Body Regeneration’ (WBR) and thought to be mediated by circulating populations of stem cells. Additional evidence comes from colony fusions: in these events, two or more individuals or colonies that are adjacent undergo interactions between tunic vessels of each, which can result in vascular anastomoses and sharing of blood (chimera formation). If the colonies are histocompatible, the anastomoses can result in somatic cell and germ-line stem cell mixing and competition, wherein stable chimeras or heritable dominant ‘winners’ outcompete ‘loser’ stem cells, called parasitism (Sabbadin and Zaniolo, 1979; Pancer et al., 1995; Stoner and Weissman, 1996; Stoner et al., 1999). Similar chimerism can be induced in recipient colonies by transplanting prospective isolated circulating cells, or stem cells, between genetically distinct colonies, further providing evidence that circulating adult stem cells, the origins of which are unknown, are the cells responsible for a stable long-term chimerism in *B. schlosseri* (Laird et al., 2005). Thus stem cells can mediate organogenesis in a single organism for life, as in humans, or can be responsible for cycles of weekly generation of clonal progeny wherein the life of the colony that they sustain is long, but the lives of individuals that make up the colony are short.

Recently, we have found that the anterior ventral area of the endostyle (the ciliated feeding hypobranchial groove, that lines the pharyngeal midline ventral floor of the adult zooid) and cells in the subendostylar sinus beneath it, harbors somatic stem cells that can contribute to a wide range of developing tissues (the EN niche; Voskoboynik et al., 2008). However, the long-term fates of these stem cells and whether stem cells are consumed by the colony-wide apoptotic event (the weekly ‘takeover’ stage of blastogenesis), or able to evade it, are unknown. If stem cells are able to evade the apoptotic stage by repeatedly cycling, this may ensure their self-preservation throughout the organism’s life and provide a paradigm for the maintenance of adult stem cells, as most adult stem cell systems (somatic and germline) are regarded sedentary.

Here, we have characterized a distinct niche for germ-line and somatic stem cells in cell aggregates that laterally line the adult endostyle (termed ‘cell-islands; CIs; Fig. 1B). We reveal cyclic, and long-term migrations of these putative stem cells, that colonize CIs in developing buds, reconstituting both soma and germ-line in each following blastogenic generation of zooids.

NIH-PA Author Manuscript

NIH-PA Author Manuscript

NIH-PA Author Manuscript

Results

The endostyle and cell islands (CIs) highly express stem cell associated markers

To characterise molecular expression signatures of the endostyle and its surrounding cells (Voskoboynik et al., 2008), we searched three EST libraries from *B. schlosseri* (Oren et al., 2007) and *Botrylloides leachi* (Rinkevich et al., 2007, 2008). We used an array of mRNA probes with sequence specificity to *Botryllus/Botrylloides*, and polyclonal antibodies (most of which were raised against *Botryllus/Botrylloides* sequences or bound specific cellular components) to detect gene products unique to the endostyle and its adjacent cells, that are implicated in developmental regulation, stem cell maintenance and cellular differentiation in other model systems (n=31, supplementary table 1). Different zones within the endostyle showed specific gene expression combinations. The anterior ventral zone 1 (z1) expressed phosphorylated *Smad2* (Fig. S1A, red arrow) indicating active TGF-β family signaling, *β-catenin* (Fig. S1B, red arrow) indicating potential Wnt signaling, and *Piwi*, a germ/somatic stem cell marker (Fig. S1, C, D, red arrows). Proliferating cell nuclear antigen (*PCNA*, Fig. S1E, red arrows) was expressed within all endostyle zones except z1, suggesting that cells within z1 and the sinus beneath it are slow dividing. Zone 2 (z2) cells expressed protein kinase C (*PKC*, Fig. S1F, red arrow). Zones 3 and 5 (z3, z5) contained cells that were *peroxidase* positive (Fig. S1G, red arrows). Zone 4 (z4) expressed the von Willebrand factor (*vWF*, Fig. S1H, red arrows; as well as z2, z6, z8 [Oren et al., 2008]), and *β-catenin* in a strip of midline cells (Fig. S1B, black arrows). Zone 6 (z6) expressed the homeodomain transcription factor and pluripotency gene *Oct4* (Fig. S1I, red arrows), the signal transduction and activator of transcription (*STAT*, Fig. S1J, red arrows) from the JAK/STAT signaling pathway and representatives of the retinoic acid (RA) signaling pathway, including retinoic acid receptor (*RAR*, Fig. S1K, red arrows), the retinaldehyde dehydrogenase-related gene (*Raldh*, Fig. S1L, red arrows) and retinoic acid inducible protease (*Trsp*, Fig. S1M, red arrows). Zones 7 and 8 (z7, z8), both of which are sites of iodine concentration and metabolism for thyroid hormone synthesis (Ogasawara et al., 1999; Hiruta et al., 2006), were not marked by any of the stem cell and developmental markers analyzed, but showed the ubiquitous expression (z1-z8) of the anti-apoptotic gene (*Bax inhibitor*, Fig. S1N, red arrows) and the structural proteins *actin* (Fig. S1O, red arrows), *laminin* (Fig. S1P, red arrows), *beta-catenin* (Fig. S1Q, red arrows) and *cadherin* (Fig. S1R, red arrows), which were expressed lengthwise along the endostyle groove.

Adult zooids harbor several pairs of compact blood cells aggregates (each termed here ‘cell island’, CI), situated lengthwise along the endostyle groove (Fig. 1, A, B) in a ventral plane to the EN (Voskoboynik et al., 2008). Each cell island is composed of few hundreds of various cell types, small and large, elongated and circular cells, single and multinucleate cells, all connected to each other through a mesh of cellular extensions, forming a globular to lengthened CI (Fig. S2). Each CI is surrounded by circulating cells and encased within the sinus epithelium (termed here the ‘cell island niche’) that connects the CI niche to the EN.

We found markers associated with germ-line and somatic stem cells within the cell islands (Fig. 2; supplementary table 1). These include *Piwi* (Fig. 2, A, B, red arrows; also documented in *Botrylloides violaceus* [Brown et al., 2009]), *alkaline-phosphatase* activity (Fig. 2C, red arrows), the germ-line marker *Vasa* (Fig. 2D, red arrows), its closely related DEAD-box RNA helicase *Pl10* (Fig. 2E, red arrows), which is highly expressed in differentiating tissues (Rosner et al., 2006) and *PCNA* (Fig. 2F, red arrows), indicating CIs as a candidate niche for stem cells and an active site for cell division. This localized expression was in contrast to low expression of stem-cell associated markers in other zooidal organs, developed buds, or the circulatory system, except for the gonads (Brown and Swalla, 2007; Brown et al., 2009; Rosner et al., 2009). CIs also expressed genes indicative of an active signaling microenvironment, e.g. FGFR (Fig. 2G, red arrows), *MAPK* (Fig. 2H, red

NIH-PA Author Manuscript

NIH-PA Author Manuscript

NIH-PA Author Manuscript

arrows), the MAP kinase signal-integrating kinase (*Mnk*, Fig. 2I, red arrows), *Rap1A* (Fig. 2J, red arrows), *Rab33* (Fig. 2K, red arrows) from the Ras oncogene family, *Slit* (Slit/Robo signaling pathway implicated in both axonal guidance and mouse hematopoietic stem cell niches, Fig. 2L, red arrows), phosphorylated *Smad1/5/8* (Fig. 2M, red arrows) indicating active bone morphogenetic protein (BMP) signaling and/or the *STAT* (JAK/STAT signaling pathway; Fig. 2N, red arrows) in a subset of cells within CIs. Both *PKC* (Fig. 2O, red arrows) and the receptor for activated PKC (*RACK*, Fig. 2P, red arrows) are expressed within CIs, as well as the zinc finger transcription factor *Cnot* (Fig. 2Q, red arrows), the anti-apoptotic gene (*Bax inhibitor 1*; Fig. 2R, red arrows), the cell adhesion protein *cadherin* (Fig. 2S, red arrow) and an orthologue of the ficolin gene containing a fibrinogen domain, which showed a heightened expression in immunologically challenged colonies (Fig. 2T, red arrow; [Oren et al., 2008]). The possibility that CIs co-express components from multiple signaling pathways (Fig. 2U) including FGF, BMP, JAK/STAT, Ras oncogene and Slit/Robo family members, is consistent with but not proof of a microenvironment for germ-line and somatic stem cells. These markers encouraged us to study the biological and transplantation properties of the CIs and the possibility of its long-term repopulation capacity, in detail.

Migratory routes and homing patterns of CI cells in vivo

We used *in vivo* cell-labeling, and time-lapse imaging to track and follow the migration patterns of resident CI cells. At early blastogenic stage A, a CI niche harbors an average of 2710±174 cells. Then, cell numbers within CI niches decrease concomitant with development to 2480±88 cells at stage B, to 1870±142 cells at stage C, 830±57 cells during early stage D and eventually emptying the aged CI niches before their degeneration as stage D progresses. During stage D, we noticed a simultaneous surge of cells into newly formed CIs and CI niches of next generation of buds. *In vivo* imaging demonstrated a gradual abandonment of cells from existing CIs via the surrounding blood sinus, as blastogenesis progressed (supplementary time lapse video 1; Fig S2). Immunhistochemistry of CIs showed a clear quantitative decline of *Piwi*$^{+}$ and *Vasa*$^{+}$ cell numbers within CIs as blastogenesis progressed, with a steep drop in cell numbers preceding the ‘take-over’ stage: 40 Piwi^{+} cells, 60 Vasa^{+} cells during stage A, to 4 Piwi^{+} cells, 20 Vasa^{+} cells during early stage D.

Next, we labeled groups of 20-60 cells from the EN niche (Vibrant Did, 665nm emission spectra; Fig. 3A; supplementary table 2) and followed their migration *in-vivo* for up to nine days throughout the whole blastogenic cycle. Labeled cells dispersed during blastogenic stages A-C throughout the zooid sinuses, proliferated and migrated towards developing tissues of the colony including primary and secondary buds (Fig. 3, A’, A”), in agreement with previous results (Voskoboynik et al., 2008). In the developing primary buds labeled cells were mainly detected in the sinuses and in CIs on contralateral sides of the newly formed endostyle (Fig. 3A’”). At 30 hours following labeling, cells from the EN lost 80% of their fluorescence intensity. High numbers of low-intensity labeled cells in the sinuses and CIs indicated the high proliferative potential of original EN niche labeled cells. We then labeled 10-50 cells *in situ* from a single anterior CI (Vibrant Did, 665nm emission spectra 1-2 CI per zooid; Fig. 3B, outlined by a dotted circle) and tracked cell’s locations and migrations using time-lapse microscopy for up to 14 days (supplementary table 3). Within three days, labeled cells migrated from anterior to posterior CI’s, to CI’s on both sides of the endostyle and to CIs in neighboring zooids (Fig. 3B’, 3B” white arrows; supplementary table 3). During early blastogenic stage D, labeled cells vacated aged CIs and were observed colonizing CIs within the new generation of buds (Fig. 3B’”, white arrows, 6 days following labeling; supplementary table 4). As new buds matured (10 days post labeling), we found labeling within the germ-line, both in immature and mature oocytes that were situated within the brooding pouch (Fig. 3, C-C’”, white arrows) as well as in the testis (Fig. 3, D-D’”,

NIH-PA Author Manuscript

NIH-PA Author Manuscript

NIH-PA Author Manuscript

white arrows). Control groups (n=3), injected with 10-50 labeled circulating blood cells (taken from colonies at blastogenic stages A-C), did not show any cell-expansions within recipient colonies or labeling within CIs or the germ-line.

To further characterize the long term cycling of candidate stem cells between niches we transplanted cells that were labeled with DiI *ex-situ* (to circumvent the possibility of DiI leakage). Cells were drawn from the EN niche of blastogenic stage C colonies (13 zooids), labeled and then introduced back into peripheral ampullae of sub-cloned colonies (n=16) and followed for up to 4 blastogenic cycles. Labeled cells circulating within the vasculature (Fig. 4 A-A") fully engrafted CIs of newly developed zooids within 6 to 10 hours following infusion. In addition, labeled cells colonized multiple tissues including the branchial sac, ampullae and siphon of recipient colonies, in cell foci, maintaining their presence there throughout blastogenesis. During stage D, a surge of labeled cells migrated into the primary buds, and reconstituted CIs and CI niches on both contralateral sides of the newly formed endostyle (Fig. 4B, 2nd cycle). The migration into developing CIs and CI niches occurred at every blastogenic cycle (Fig. 4B', 3rd cycle) and was documented throughout 4 blastogenic cycles (Fig. 4B", 4th cycle). Labeled cells within CIs gradually lost their fluorescence intensity, most likely due to cell proliferation (see Fig. 4B vs. 4B', 4B"), and were undetectable after 4 blastogenic cycles. With each blastogenic cycle, similar migratory routes were established by CI cells into the branchial sac, ampullae and siphons of developing buds (Fig. 4, C-C""), a subset of which repeatedly reconstituted new CIs, as buds matured. Labeled CI-cells that maintained foci within the siphon, branchial sac and ampullae did not express stem cell associated genes (Fig. 4, D-D""). Again, we found that control groups of labeled circulating blood cells, taken from the vasculature of colonies at blastogenic stages A-C (n=3), did not migrate to CIs, remained within the circulation and subsequently vanished from host colonies within a few blastogenic cycles.

Labeled blood cells that were taken from the vasculature of stage D colonies (a stage where stem cell mobilization is at its highest), engrafted CIs within 6 to 10 hours following transplantation (Fig. S3). This observation is consistent with our hypothesis that self-renewing cells engage in migration during blastogenic stage D and suggests the presence of a cell-intrinsic cue/s that guides stem cells to CIs. *In-vivo* time-lapse imaging of labeled cells taken from blastogenic stage D during 18 days (3 consecutive blastogenic cycles) revealed similar surges of engraftments into CIs taking place during stage D within 6-10 hours from infusion (Fig. S3, C, D). Labeled cells taken from stage D that migrated into CIs expressed *Piwi* (Fig. S3, E1-E5), *Vasa* (Fig. S3, F1-F5) and *Pl10* (Fig. S3, G1-G5). In addition, a subset of cells expressed *FGFR* (Fig. S3, H1-H5) and *Smad1/5/8* (Fig. S3, I1-I5) indicating presence of FGF and BMP signaling within the niche, and *cadherin* protein (Fig. S3, J1-J5). These outcomes are consistent with previous observations in which experimentally separated blood vessels from colonies of *Botryllus schlosseri* successfully regenerate, only if amputated during stage D (Voskoboynik et al., 2007). It also suggests that stem cell mobilization into the vasculature and/or its rate may be a prerequisite for successful generation/regeneration to take place.

Although we are technically unable to determine the identity of the specific cells within CIs that have repopulating activity, these experiments demonstrate that CIs harbor cells which: 1) Migrate from EN; 2) maintain long-term repopulation capacity, documented here for up to four consecutive colony generations; 3) contribute, in each blastogenic cycle, to multiple tissue sites within the colony; 4) contribute to the germ-line 5) are the cells-of-origin for new CIs and most likely all future CIs.

NIH-PA Author Manuscript

NIH-PA Author Manuscript

NIH-PA Author Manuscript

Transplantation of CIs induces long-term germ-line and somatic cell chimerism in host tissues

Independently, we evaluated the ability of CI-cells to induce long-term chimerism following their transplantation into genetically distinct colonies. Cells from 1-3 CIs were transplanted into recipient colonies (supplementary table 4). Equal cell numbers from the colony vasculature (including ampullae) served as a control group. Both somatic and germ-line tissues (if sexually mature) were harvested after 2-4 months (up to 16 blastogenic cycles) following transplantation. Chimerism was assayed using amplified fragment length polymorphism (AFLP) or microsatellite analysis, which identifies donor genetic markers in recipient tissues. Chimerism was determined when the genetic fingerprints of the donor were identified in the host, either exclusively or with host fingerprints. Engraftment of donor CIs into sexually mature recipient colonies led to 100% of recipient colonies showing some chimerism (3/3), with 43% chimerism detected in somatic tissues (10 Out of 23 somatic DNA samples) and 84% chimerism detected in germline tissues (11 out of 13 germline DNA samples; tested by AFLP; Fig. 5, A, B; Fig. S4, supplementary table 4), whereas recipient colonies that were injected with equivalent cell numbers from the vasculature/ ampullae showed no sign of chimerism at either sampling dates (supplementary table 4, Fig. S4). Moreover, in all recipient colonies that have been transplanted with CI cells but which did not develop gonads by the time of sampling, chimerism was completely absent (supplementary table 4). While not proving a common precursor to germ-line and somatic lineages, these outcomes establish the place-of-origin for germline stem cells within the CIs.

Knockdown of Cadherin and Piwi

Labeled cells transiting the colony circulation during stage D, expressed *Piwi* (Fig. S5, A-E), *Vasa* (Fig. S5, F-J) and *PCNA* protein (Fig. S5, K-O), similar to their expression patterns within CIs, but showed minimal *cadherin* expression, if any (Fig. S5, P-T). To test whether down-regulation/expression of *cadherin* might play a functional role in the retention of cells to CIs or their re-trafficking into the colony circulation, we knocked-down *cadherin* using sequence specific siRNAs (Rosner et al., 2007).

Ten days of *cadherin* RNAi administration resulted in *cadherin* protein level reduction (Fig. 6A; Rosner et al., 2007), and disorganized morphology of the endostyle and CIs (Fig. 6B). The endostyle appeared loose, with scattered cells (3-4 μm in diameter, Fig. 6A,B, arrowheads) mainly at the endostyle ventral lip, which expressed *PCNA* (Fig. 6C, arrowheads) and *Oct4* (Fig. 6D, arrowheads). CIs appeared empty (Fig. 6E-H) compared to control colonies (Fig. 6E'-H'), with minimal *Piwi*$^+$ (Fig. 6E), *Vasa*$^+$ (Fig. 6F) and *Pl10*$^+$ (Fig. 6G) cells, and reduced expressions of *Smad1/5/8* (Fig. 6H) and *FGFR* (Y.R. personal observations). We then checked whether vacancy of CIs resulted from putative stem cells re-trafficking to the circulation, and found abundant *Piwi*$^+$ (Fig. 6, I1-I3, arrowheads), *Vasa*$^+$ (Fig. 6, J1-J3, arrowheads), *Pl10*$^+$ (Fig. 6, K1-K3, arrowheads) and *PCNA*$^+$ (Fig. 6, L1-L3, arrowheads) in cells within the colony vasculature, similar to the stem cell distributions found during 6-10 hour window of blastogenic stage D.

Conversely, knockdown of *Piwi* did not lead to aberrant morphology (Fig. S6A), or differences in the expression of structural genes (sub-membrane *β-catenin*$^+$, *cadherin*$^+$, *laminin*$^+$ and *actin*$^+$, Fig. S6, B-E, respectively) within the endostyle and CIs. *Piwi*-knockdown colonies sustained normal blastogenesis, developed primary and secondary palleal buds, albeit at a slower pace and progressed through the 'take-over' phase similar to control ramets. However, *Piwi*$^+$ cells were absent from mature and developing CIs (Fig. 7A). Likewise, reduced numbers of *Vasa*$^+$ (Fig. 7B), *Pl10*$^+$ (Fig. 7C) and *PCNA*$^+$ (Fig. 7D) cells were recorded within mature and developing CIs and from the circulation of *Piwi*-knockdown colonies.

NIH-PA Author Manuscript

NIH-PA Author Manuscript

NIH-PA Author Manuscript

We then checked if absence of *Piwi*$^+$ cells would alter regeneration. Botryllid ascidians commonly regenerate adult zooids from peripheral blood vessels following their separation from the colony; a process termed Whole Body Regeneration (WBR; Oka and Watanabe, 1957; 1959; Rinkevich et al., 1995, 2007, 2010; Voskoboynik et al., 2007; Brown et al., 2009). Surgically separated blood vessels from RNAi treated *B. leachi* colonies showed a decline in *Piwi*$^+$ cell numbers by an order of magnitude, from 1073 cells/mm^2 of same stage regenerating controls to 77 cells/mm^2 (Fig. 7, E, F compare to F'). RNAi treated blood vessels exhibited morphological events that were stereotypic of early *B. leachi* WBR stages, including shrinkage within the tunic, anastomosis with other blood vessels and migration of blood vessels within the tunic to form blood vessel lacunae (Rinkevich et al., 2007; Brown et al., 2009). However, regenerating buds were completely absent from RNAi treated vessels and functional zooids were never formed (Fig. 7G compare to G'). Histological analyses revealed multiple sites within the vascular in which buds normally regenerate, but which were devoid of buds (Fig. 7H compared to H'; buds usually appear from days 3-4).

We conclude that, while *cadherin* is essential in confining putative stem cells to the CIs (its loss is concurrent with the early dislocation of stem cells from the niche and their re-trafficking to the colony circulation), *Piwi* knockdown results in colonies deficient in functional stem cells, leading to regeneration arrest.

Discussion

Stem cell niches are defined as anatomical compartments that harbor and maintain stem cells and regulate their fates *in vivo* via specific spatiotemporal inputs (Jones and Wagers, 2008). This anatomical site may co-develop either with sustained stem cells or through ontogeny, independent of host stem cells (Morrison and Spradling, 2008). It has been suggested that in botryllid ascidians, stem cells mediate a myriad of biological events, including aestivation, hibernation, blastogenesis, 'take-over', colonial chimerism, somatic and germ-line parasitism and diverse regeneration phenomena (Oka and Watanabe, 1957; 1959; Pancer et al., 1995; Rinkevich et al., 1995, 2007, 2010; Stoner et al., 1999; Lauzon et al., 2002; Voskoboynik et al., 2007; Brown et al., 2009) and serve as evolutionary units of natural selection (Weissman 2000; Laird et al., 2005). While the life span of botryllid colonies may exceed several years (Rinkevich et al., 1992; colonies of *Botryllus schlosseri* have been maintained under laboratory conditions for up to 13 years [A.V and K.J.I, unpublished observations]). Each zooid within the colony cycles on a weekly basis and is resorbed by a colony-wide apoptotic and phagocytic wave (Lauzon et al., 1992). This portrait of a transient soma (possessing transient stem cell niches) should reflect both the status and strategy of the adult stem cells, disparate from other model cases. In the *Drosophila* testis (Leatherman and Dinardo, 2010), somatic stem cells maintain long-term supportive capacity for germ-line stem cells. Here we propose an alternative mechanism in which germ-line and somatic stem cells continuously migrate (on a weekly basis) between aged or damaged niches to newly formed niches as a means of facilitating their long-term fates (see 'Graphical Abstract').

This cellular migration from CIs to CIs through the vasculature at stage D is mimicked in colonies where cadherin expression has been silenced, suggesting that the migration mechanism of putative stem cells into new niches may be regulated, or partly regulated, through cells that use calcium-dependant adhesions. The simplest model of this is that without cadherin mediated cell:cell adhesions, the architecture of the niche is disrupted, allowing formerly bound stem cells to escape.

Within CIs, stem cells and their descendants proliferate (as judged by *PCNA* expression and decrease in DiI label over time) and express a panel of stem cell-associated markers (*Piwi,*

NIH-PA Author Manuscript

NIH-PA Author Manuscript

NIH-PA Author Manuscript

Vasa, alkaline-phosphatase, *Nanos* [Sunanaga et al., 2008], *Pl10*) indicative of germ-line stem cells. Both germ-line chimerism (the presence of germ cells within gonads, derived from more than a single individual) and germ-line parasitism (takeover of host gonads by foreign germ cells; Sabbadin and Zaniolo, 1979; Rinkevich et al., 1992; Pancer et al., 1995; Stoner and Weissman, 1996; Stoner et al., 1999) commonly follow vascular fusions between genetically distinct colonies and are presumed to involve circulating germ-line stem/progenitor cells. Indeed, *in-vivo* tracing of CI-cells revealed Vybrant DiD labeling within both male and female gonads of the colony. Furthermore, our CI transplantation induced long-term germ-line chimerism in all sexually mature recipient colonies, demonstrating CIs as the site-of-origin for germ-line stem cells. In some of these CI transplanted colonies somatic chimerism was also detected, all somatic samples include CIs, which could be the origin for the somatic chimerism detected. CIs also activate several signaling pathways (JAK/STAT, BMP, FGF, MAPK, PKC, Ras oncogene and Slit/Robo), highlighting this tissue as signaling centers that possibly instruct stem cells to other progeny routes. In agreement with this, *in vivo* DiI-labeled cells originated from the EN migrate to CI niches and contributed to numerous colony sites during blastogenesis, including siphon, branchial sac, ampullae and blood vessels in addition to their participation in populating new CIs and the germ-line. At the end of each blastogenic cycle (one week), putative stem cells are not consumed by the apoptotic wave but continue their journey through the colonial vasculature to newly developed CI sites of the next zooidal generation, in weekly and cyclic routes (followed in the present work for up to 4 blastogenic cycles). Still, the number of CI niches within a colony is an outcome of the number of zooids and emerged palleal buds in each blastogenic cycle, so the decision of a defined stem cell to which specific CI it homes or which colony region it contributes to, is still unknown. Indeed, colonies transplanted with CI cells display chimerism after 98 days within some but not all zooids, and may account for a selective migration of stem cells. In solitary tunicates, migration of neural precursors during the metamorphic transition from larva to adult has recently been documented to account for the origin of the adult central nervous system cells (Horie et al., 2011), implying stem cell migrations as a possible adaptive mechanism that facilitated the life history transitions (metamorphosis, blastogenesis, whole body regeneration and the resurgence from hibernation/aestivation).

The complex system of repeated migrations of putative stem cells between niches, as emerged in the botryllid ascidians system, is an efficient tool allowing stem cells to escape senescence imposed by the short somatic lifespan of individual zooids, thereby enabling their continuous propagation and function in somatic/germ-line generation and regeneration throughout the organism's life. The identification of the exact cells within CIs that have repopulating activities would require transgenic assays for genetic lineage tracing and/or generating antibody libraries against surface molecules for its use in flow cytometry, both of which are currently unavailable in botryllid ascidians and we hope to be able to address it in the future. Characterization of the CI niche, including the identities of resident stem cells, their varied differentiation routes and migration mechanisms will most likely contribute to our understanding of the variations (and commonalities) in stem cell systems portrayed within the animal kingdom.

Experimental Procedures

Colony development and husbandry

Colonies of *Botryllus schlosseri* and *Botrylloides leachi* were collected from shallow waters along the Monterey Bay marina, USA and the Israeli Mediterranean coast, respectively, and were carefully peeled-off the underlying surfaces of stones with industrial razor blades. To minimize tissue damage of *B. leachi* colonies collected from the wild, each peeled sample included an attached thin layer of calcareous substrate. Isolated colonies were individually

NIH-PA Author Manuscript

NIH-PA Author Manuscript

NIH-PA Author Manuscript

tied with fine cotton thread onto 5×7.5cm glass slides and cultured in 17-liter tanks in a standing seawater system at 20°C. Within several days, the colonies glided, completely or partially, from their original calcareous substrate onto the glass slides. Colonies and their substrates were cleaned weekly with industrial razor blades and fine brushes.

The endostyle

The endostyle is a longitudinal ciliated feeding groove of right and left symmetrically opposed halves that extend anteroposteriorly on the ventral wall of the pharynx and lines the pharyngeal midline ventral floor of all extant tunicates, cephalochordates, hemichordates and the larvae of ammocetes (Rychel et al., 2006). While its traditional function in tunicates is secreting mucus that traps food particles, the complex morphological and cellular structures of the endostyle suggest more than just a mucus-processing organ (Compere and Godeaux, 1997). The endostyle harbors specialized secretory cells that bind iodine (Thorpe and Thorndyke, 1975) and these may represent the primitive antecedent to the vertebrate thyroid gland (Rychel et al., 2006). In botryllid ascidians (Fig. 1, A, B), the endostyle develops as a 0.7 mm long and 75 μm in diameter rod-shaped grooved ridge, running the length of the zooid, forming a seam along the ventral margin of the pharyngeal basket with a connection to the pharynx via a duct. With its longitudinally ciliated and glandular tracks, this organ has been classically defined on the cross-section plane by 7 pairs of distinct functional units called ‘zones’ (Burighel and Cloney, 1997) termed z2-z8; numbered bilaterally from the midventral most zone (z1) and extending dorsolateral (Fig. 2). A ninth zone (z9), lateral to z8 has occasionally been described, as well as subdivisions of zones into additional sub-zones, but are not represented here. The eight pairs of endostyle zones include three supporting zones (zones 1, 3, 5; Fig. 2U), three-pairs of glandular zones (zones 2, 4, 6), and two-pairs of iodine-binding zones (Burighel and Cloney, 1997; zones 7 and 8; Fig. 2U). All endostyle zones are bathed in a large blood sinus (Burighel and Brunetti, 1971). The subendostylar sinus is located beneath the anterior ventral region of the endostyle zones 1 and 2, termed as the endostyle niche (EN; Voskoboynik et al., 2008).

Regeneration assay

Under a dissecting microscope, marginal ampullae and fragments of blood vessels were separated from colonies of *B. leachi* growing on glass slides, using an industrial razor blade and a fine tungsten needle. Then, dissected colonies were removed from the slides and attached onto other slides. The leftover blood vessel fragments were cut into smaller fragments using a fine tungsten needle and left to regenerate in Petri dishes containing filtered seawater. Fragments were monitored daily under a dissecting microscope and photographed with a Supercam camera (Applitec, Holon, Israel).

In situ hybridization

B. leachi and *B. schlosseri* colonies were fixed overnight in 4% paraformaldehyde, gradually dehydrated in methanol (70-100%), embedded in paraffin wax and cut into 4-5μm sections. Sequence-specific primers that were used to obtain sense and antisense DIG-labeled RNA probes are listed bellow, and were synthesized using DIG RNA labeling kit (SP6/T7, Roche). Hybridization of probes to tissue sections was performed according to Breitschopf et al. (1992) for paraffin-embedded tissues. DIG-labeled RNAs on samples were revealed using anti-DIG antibody (Roche). Samples were observed under Leica DMIRE2 inverted microscope and photographed with a Leica FX300 camera.

	Homologue name	5’ primer	3’ primer	Seq. length
1	STAT	5’ AGACTCAGCTCCGCGTTTG 3’	5’ AATCATTTGGCAGAACGGAC 3’	454bp
2	Slit	5’ GGTTAATCGGCAGTCGCAAAG 3’	5’ GGCCTCAATAAATTACGTGTGC 3’	453bp

NIH-PA Author Manuscript

NIH-PA Author Manuscript

NIH-PA Author Manuscript

3	Rap1A	5’ CTGTTAGGGCTGAGCATCATAG 3’	5’ TGGCAAGACAATGGAATAACTG 3’	174bp
4	Rab33	5’ CGCAATATTAGTGTCCACATGG 3’	5’ TCCTACTCGAACTGAAGCCAC 3’	316bp
5	RAR	5’ TCGACGCTTTCGGGCATAC 3’	5’ AAGACGGCAAAGCGGGAGAG 3’	808bp
6	Raldh	5’ AGAATTTCCTTGGAGCTTGG 3’	5’ ACCCTGTTCAATGTCGCTG 3’	337bp
7	Mnk2	5’ ATGTGGTGAGGATTGTGGATG 3’	5’ AATCGTGAATGTGGCTGAAGAC 3’	475bp
8	Trsp	5’ GGTGTGGTGGATCTCTCATTC 3’	5’ GTGTCTTCGGCAGGCAAATC 3’	336bp
9	Piwi	5’ CATGGTCGGTGGAAACAAGG 3’	5’ AAACGCAGCGACGGACCTTC 3’	571bp
10	Bax inhibitor 1	5’ AAATGAAATCTATGGCACAGCG 3’	5’ TGACTGCCTTTATGACAACCTC 3’	578bp
11	Vasa	5’ TTCCAAGGACGGCACGTTGG 3’	5’ ACGTTTGATTGAACACACGG 3’	576bp
12	Cadherin	5’ AGACGTCAAGCGGCTATGAT 3’	5’ CCCTTCGTATAACATACCGG 3’	450bp
13	Pl10	5’ CTTGTCGATCTCCTGATGGA 3’	5’ GAGCCTTCCAGGTTACGCAAG 3’	576bp
14	Actin	5’ GAAATCGTGCCGTGACATCAAAG 3’	5’ GCGGTGATTCCCTTCTGCATAC 3’	338bp
15	RACK	5’ CCATTGCGGACGAAGGTCATAG 3’	5’ AAAGCGTTTGCCCATCTGATG 3’	477bp
16	Cnot	5’ TTCTCCGTAACGATTCAACTTG 3’	5’ GGGTATTTGTCATGTTTCTTGC 3’	469bp
17	vWF	5’ GTTAGGAGTGTCGCTGCAGGAG 3’	5’ GATGCTGTCCCGAATACGAGTG 3’	320bp
18	Ficolin	5’ TGGTCTCGGCGCAATTTC 3’	5’ AAGACGCGAAGCTGTGCAATG 3’	450bp

Histology and immunohistochemistry

B. leachi and *B. schlosseri* colonies were fixed in Bouin’s solution for 1-2h, dehydrated in graded ethanol series (70-100%) and butanol, and embedded in paraffin wax. Serial cross sections (4-5μm) were cut by hand-operated microtome (Leica, Nussloch, Germany) and stained with alum hematoxylin and eosin for general morphology.

For immunostaining, sections were attached to SuperFrost Plus microscope slides (Menzel-Glazer), dewaxed and its antigen retrieved (microwave, 480 W, 30min in 10mM citrate buffer [600ml, pH 6.0]). After a 5min cooling period, 1L of distilled water was added and the slides were incubated for additional 10min at room temperature, followed by several washes with TBS. Nonspecific binding sites were blocked by incubation in 1% BSA (MP Biomedicals) in 50 mM TBS for 14-16h at room temperature. The slides were washed with TBS for 5min and stained with one of the following antibodies: rabbit anti *Bl-Piwi* polyclonals (1:6000 in TBS containing 1% BSA); rabbit anti *Bs-Pl10* polyclonals (1:4000 in TBS containing 1% BSA); rabbit anti *PCNA* monoclonal (Santa Cruz; 1:100 in TBS containing 1% BSA); rabbit anti phosphorylated Smad 1/5/8 polyclonals (Cell signaling; 1:200 in TBS containing 1% BSA), rabbit anti phosphorylated Smad 2 polyclonals (Cell signaling; 1:200 in TBS containing 1% BSA), rabbit anti Oct 4 polyclonals (Cell signaling; 1:100 in TBS containing 1% BSA), rabbit anti flg (*FGFR*) polyclonals (Santa Cruz; 1:100 in TBS containing 1% BSA), rabbit anti actin polyclonals (Santa Cruz; 1:100 in TBS containing 1% BSA) for 2h at room temperature, followed by 14-16h incubation at 4°C. After washing with TBS for 5min × 3, alkaline phosphatase-conjugated goat anti-rabbit (Jackson laboratories; 1:10,000 in TBS containing 1% BSA) was added as secondary antibody. Sections were incubated for 1h-1.5h and washed with TBS for 5min × 3. Staining reaction employed a BCIP/NBT color solution. For fluorescent staining, Cy2 or Cy3-conjugated goat anti-rabbit antibodies were used (Jackson laboratories; 1:100 in TBS containing 1% BSA). For detection of nuclei, DAPI was dissolved in TBS to a concentration of 200μg/ml and was incubated with slides for 10-15min, followed by an additional 5min wash. Control and experimental sections were mounted with Hydromount (National Diagnostics) or Fluoromount-G (SoutherBiotech) and photographed with Leica FX300 camera.

NIH-PA Author Manuscript

NIH-PA Author Manuscript

NIH-PA Author Manuscript

Cell counting in CI-niche and CIs

Subclones of *B. schlosseri* colony systems at blastogenic stages A-D (4 colonies per blastogenic stage, 3-4 zooids per colony), were fixed and then embedded in paraplast. Serial sections of 10 um were placed on microscopic slides in sequential order, and stained with alum hematoxylin and eosin for general morphology. Cell counting within CI niches included CI and surrounding circulating blood cells.

DiI staining of *Botryllus* blood cells

CellTracker CM-DiI (Molecular Probes; C7000) was used for labeling of *B. schlosseri* blood cells as it shows no cytotoxicity, has a photo-stable fluorescence, stains entire cells without leakage (Y.R. and CR unpublished observations) and remains stable after fixation and paraffin embedding procedures.

Stock solutions (50μg/μl) were prepared by dissolving CM-DiI in ethanol, according to the manufacture's protocol. Immediately before usage, a 1-2 μl DiI stock solution was diluted in 1ml TCM containing *Botryllus* blood cells and incubated for 10-15min at room temperature, then further diluted in 13ml TCM to wash excess stain. Labeled cells were further centrifuged at 1500rpm for 15min. The supernatant was fully removed and the pellet was re-suspended in 20-40μl TCM. Stained blood cells were visualized under a fluorescent microscope (Olympus BX-50, Germany) equipped with an excitation filter of 550nm wavelength and a barrier filter of 579nm.

Alternatively, blood cells were drawn from *Botryllus* at the base of 13 blastogenic stage C zooidal endostyles (total of 4600 cells) and stained with DiI. Cells were washed in TCM (to dilute any unbound label) and injected into the ampullae of recipient stage C *Botryllus* colonies (16 zooids). As a control, blood cells were drawn from the ampullae of stage C *Botryllus* colonies (6700 cells) stained with DiI and injected into the ampullae of recipient stage C colonies (48 zooids, 3 colonies). Colonies where monitored for three to four consecutive blastogenic generations.

Injections of *Botryllus* blood cells

Recipient colonies were pre-cleaned and immersed in filtered seawater (0.2μm). Labeled cells were drawn into a glass capillary tube (KIMBLE products, KIMAX-51, U.S.A) pre-stretched using a capillary-stretcher apparatus (Narishige, Japan) and injected (~10μl volume/injection) intra-ampullae into a firmly attached subclone-recipient colony using a manual micro-injector and micro-manipulator (Narishige, Japan). Visualization of labeled cells inside the recipient colony was confirmed using a fluorescence microscope (Olympus BX-50).

In vivo Vybrant DiD fluorescent cell labeling assay

We used Vybrant DiD, a carbocyanine lipophilic membrane fluorescent stain (emission-665nm; Molecular Probes, Eugene OR USA) for *in vivo* cell labeling. Vybrant DiD was diluted in a tunicate saline buffer (TS; Negm et al., 1991) and used to label cells in one of the sites: ENs, CIs and ampullae. From the EN we collected cells that were located on the anterior ventral region of the endostyle epithelium (mainly lymphocyte like cells from the subendostylar sinus). Some *Botryllus* colonies have high natural fluorescent backgrounds in the 501nm and 565nm emissions spectra (Fitc and Dsred) and a low background in the 665nm emission spectra (Cy5). Therefore we chose the Vybrant DID dye (Cy5) which diffuses laterally to stain the entire cell and fluorescents weakly until incorporated into a membrane. This dye doesn't leak from cell to cell, shows little or no toxicity, and is stable for at least 120 hours. Thirty hours following labeling, cells that originated in the endostyle niche lost 80% of their fluorescence intensity. At this time frame,

NIH-PA Author Manuscript

NIH-PA Author Manuscript

NIH-PA Author Manuscript

cells from the ampullae did not lose their fluorescence intensity. The constant fluorescence and no proliferation and expansion of labeled cells in the ampullae negate the possibility of leaking of the lipophilic dye from labeled cells to other cells. We therefore conclude that no intercellular transfer of stain between cells occurred in our experiments and that proliferation of EN labeled cells observed is due to cell proliferation.

Vybrant DiD labeling of CIs cells

Cells were labeled *in situ* using Vybrant DiD dye solution (emission 665 nm; Molecular Probes) in three colonies in the zooid anterior cell island. One-two cell islands were labeled per every studied zooid, 2-4 zooids were labeled in each experimental colony. Colony #1, at the time of labeling was at blastogenic stage A and comprised 14 zooids, CIs in 4 different zooids were labeled. Colony #2 at the time of labeling was at blastogenic stage B and comprised 9 zooids, CIs in 4 different zooids were labeled. Colony #3 at the time of labeling was at blastogenic stage B and comprised 8 zooids, CIs in 2 different zooids were labeled.

Imaging

Time lapse imaging was performed by automated microscopy (ImageXpress, Molecular devices Corp., Palo Alto, CA). Phase contrast images were taken every 30 minutes at 10X magnification for several days. Image acquisition, processing and analysis was performed by Leica MM AF Intergrated Imaging System (Leica, Microsystems Inc). Following labeling, phase contrast images and fluorescent images (cy5, maximum emission at 670nm) at varying magnifications were performed every 1-2 days during the first 6 days following labeling and every 4 to 5 days thereafter (days 6-15).

RNAi treatment

Custom designed siRNAs were purchased from Ambion (www.ambion.com) based on two regions from the full-length sequence of *Piwi*. siRNA sequence 295169: Sense: GGUGGACUAUUCUUGAAUAtt, Antisense: UAUUCAAGAAUAGUCCACCtt. siRNA; sequence 295170: Sense: CCAUCAGUUUCUUUGACUAtt, Antisense: UAGUCAAAGAAACUGAUGGtt, in addition to an unrelated control siRNA. Sub-clones from different *B. schlosseri* genotypes were soaked for 4-10 days in 50ml filtered seawater containing 20nM siRNAs. Fresh medium containing 20nM siRNA was changed every other day until termination of experiment. All RNAi treatments were done in a 20°C culture room. Colonies were monitored daily under a dissecting microscope and photographed with a Supercam camera (Applitec, Holon, Israel). Sequence specific siRNAs against *cadherin* was designed as follows: CAD127s 5′-AATGGACATAGATCTGTCGGTCCTGTCTC-3′ and CAD127a 5′-AAACCGACAGATCTATGTCCACCTGTCTC-3′. CAD2686s 5′-AATAACATACCGGCGAGACGACCTGTCTC-3′ and CAD2686a 5′-AATCGTCTCGCCGGTATGTTACCTGTCTC-3′. CAD1000s 5′-AAATAGTTGAGATCGTCGCCGCCTGTCTC-3′ and CAD1000a 5′-AACGGCGACGATCTCAACTATCCTGTCTC-3′. CAD726s 5′-AAACAGGATCCTCAGTTGGATCCTGTCT-3′ and CAD726a 5′-AAATCCAACTGAGGATCCTGTCCTGTCTC-3′. Control5 5′-AACCATCTGCTAATCTGTAACCCTGTCTC-3′ and Control3 5′-AAGTTACAGATTAGCAGATGGCCTGTCTC-3′.

Transplantation Experiments

Tested tissues (cell islands or ampullae) were dissected from donor colonies (blastogenic stage A or B) and transplanted into the recipient colony zooids (blastogenic stage A). Tissue dissections and transplantations were performed under a Wild Heerbrugg, microscope, model 160272.

NIH-PA Author Manuscript

NIH-PA Author Manuscript

NIH-PA Author Manuscript

Genotyping

Somatic and germ-line tissues (when available) were collected at intervals, 1 to 4 months following transplantation (colonies were starved for at least 16 hours prior to sample collections). Samples were dissected and flash-frozen in liquid nitrogen. DNA was extracted and the samples were screened for specific genotype-fingerprints using amplified fragment length polymorphism (AFLP) typing. DNA samples from transplanted subclones were compared with DNA samples of donor and recipient. To ensure consistency of AFLP fingerprints, some experiments were repeated twice. For the initial amplification, 2 different primer sets were used for each sample from the following options: EcoRI tag/MseI agg, EcoR1 tcg/ MseI aga, EcoRI tcg/MseI agg, EcoR tag/MseI act. We concluded that individuals have a “genetic chimerism” when the AFLP revealed the presence of the amplified fragments or genetic markers (DNA fingerprints) of the donor.

Microsatellite Assay

Microsatellite reactions were carried out in Illustra Hot Start Ready-To-Go PCR Beads (GeHealthcare #28-9006-53). Each bead contains 2.5 units PuReTaqDNA polymerase, 10mM tris-HCl 50mM KCl, 1.5mM MgCl, 200μM of each dNTP and BSA. Fluorescent labeled primers were synthesized by Operon Technologies.

Primers were synthesized and used pairwise as follows,

PB29F (6-FAM):TTGTGTGGGGCGACGCTT, PB29R; GGAACTCGCAATCCACTG

811F (NED): TCAACTCGATGGACT, 811R: CGACATTGTGGGCGAGTAC

PB49F(VIC):GGAGACATGTTACTGTGTACTGCG,
PB49R;TATCGCTCCAAGTTGACTTGG

PB41F(PET):CACGTATCGGTACCGAGTTGTCTG,

PB41R:CTTATTCTGAACTTGATTTCATTGTGCG

Illustra beads were reconstituted with H_2O to 25μl final volume, 1.0μl 10uM of each primer per primer pair, and 50ng template genomic DNA. Amplification was completed on an MJ Research Thermal Cycler PTC-200 as follows: Initial denaturization for 5 min at 95°C, followed by 36 cycles of 95° for 1 min, 56° for 1 min, 72° for 1 min, followed by a final extension of 72° for 30 min. 5 μl of the PCR product from each primer set was combined in a single well in a 96-well plate and sent to MCLAB (San Francisco, CA) for microsatellite analysis.

The fluorescent labeled PCR products were sequenced by MCLAB. DNA from most of the samples were amplified and run in duplicates (or triplicates) to validate repeatability. The similarities between duplicated fingerprints were found to be higher than 98%.

Each individual colony was typed by two Microsatellite loci. Allele identification and genotyping were determined directly from the electropherogram using GeneMarker (Soft Genetics), State College, PA).

Supplementary Material

Refer to Web version on PubMed Central for supplementary material.

Acknowledgments

The authors would like to thank Chris Patton for his invaluable technical advice and imaging. This study was supported by a grant from the United States-Israel Bi-National Science Foundation (2003-010 to BR and ILW),

NIH-PA Author Manuscript

NIH-PA Author Manuscript

NIH-PA Author Manuscript

from the Israel Academy of Science (68/10 to BR; 1342/08 to JD), and by NIH grants 1R56AI089968-01, RO1GM100315-01 and 1R01AG037968-01 to ILW. Y.R. is supported by the Human Frontier Science Program (HFSP) Long Term Fellowship, the Machiah Foundation Fellowship and the Siebel foundation (1119368-104-GHBJI).

References and notes

Brown FD, Swalla BJ. Vasa expression in a colonial ascidian, Botrylloides violaceus. Evol Dev. 2007; 9:165–177. [PubMed: 17371399]

Brown FD, Keeling EL, Le AD, Swalla BJ. Whole body regeneration in a colonial ascidian, *Botrylloides violaceus*. J Exp Zool B Mol Dev Evol. 2009; 312:885–900. [PubMed: 19588490]

Burighel P, Brunetti R. The circulatory system in the blastozooids of the colonial ascidian *Botryllus schlosseri* (Pallas). Boll Zool. 1971; 38:278–289.

Burighel, PA.; Cloney, RA. Microscopic anatomy of invertebrates. Wiley-Liss, Inc.; New York: 1997. p. 221-347.

Compere P, Godeaux JEA. On endostyle ultrastructure in two new species of doliolid-like tunicates. Mar Biol. 1997; 128:447–453.

Horie T, Shinki R, Ogura Y, Kusakabe TG, Satoh N, Sasakura Y. Ependymal cells of chordate larvae are stem-like cells that form the adult nervous system. Nature. 2011; 469:525–528. [PubMed: 21196932]

Laird DJ, De Tomaso AW, Weissman IL. Stem cells are units of natural selection in a colonial ascidian. Cell. 123:1351–1360. [PubMed: 16377573]

Lauzon RJ, Ishizuka KJ, Weissman IL. A cyclical, developmentally-regulated death phenomenon in a colonial urochordate. Dev Dyn. 1992; 194:71–83. [PubMed: 1421521]

Lauzon RJ, Ishizuka KJ, Weissman IL. Cyclical generation and degeneration of organs in a colonial urochordate involves crosstalk between old and new: a model for development and regeneration. Dev Biol. 2002; 249:333–348. [PubMed: 12221010]

Manni, Zaniolo G, Cima F, Burighel P, Ballarin L. *Botryllus schlosseri*: a model ascidian for the study of asexual reproduction. Dev Dyn. 2007; 236:335–352. [PubMed: 17191252]

Morrison SJ, Spradling AC. Stem cells and niches: mechanisms that promote stem cell maintenance throughout life. Cell. 2008; 132:598–611. [PubMed: 18295578]

Negm HI, Mansour MH, Cooper EL. Identification and structural characterization of Lyt-1 glycoproteins from tunicate hemocytes and mouse thymocytes. Comp Biochem Physiol B. 1991; 99:741–749. [PubMed: 1790669]

Ogasawara M, Di Lauro R, Satoh N. Ascidian homologs of mammalian thyroid peroxidase genes are expressed in the thyroid-equivalent region of the endostyle. J Exp Zool. 1999; 285:158–169. [PubMed: 10440727]

Oka H, Watanabe H. Vascular budding, a new type of budding in Botryllus. Biol Bull. 1957; 112:225–240.

Oka H, Watanabe H. Vascular budding in Botrylloides. Biol Bull. 1959; 117:340–346.

Oren M, Douek J, Fishelson Z, Rinkevich B. Identification of immune-relevant genes in histoincompatible rejecting colonies of the tunicate *Botryllus schlosseri*. Dev Comp Immunol. 2007; 31:889–902. [PubMed: 17287019]

Oren M, Escande ML, Paz G, Fishelson Z, Rinkevich B. Urochordate histoincompatible interactions activate vertebrate-like coagulation system components. PLoS One. 2008; 3:e3123. [PubMed: 18769590]

Rinkevich B, Shlemberg Z, Fishelson L. Whole-body protochordate regeneration from totipotent blood cells. Proc Natl Acad Sci USA. 1995; 92:7695–7699. [PubMed: 11607571]

Rinkevich B, Lauzon RJ, Brown BW, Weissman IL. Evidence for a programmed life span in a colonial protochordate. Proc Natl Acad Sci USA. 1992; 89:3546–3550. [PubMed: 1565651]

Rinkevich Y, Douek J, Haber O, Rinkevich B, Reshef R. Urochordate whole body regeneration inaugurates a diverse innate immune signaling profile. Dev Biol. 2007; 312:131–146. [PubMed: 17964563]

NIH-PA Author Manuscript

NIH-PA Author Manuscript

NIH-PA Author Manuscript

Rinkevich Y, Paz G, Rinkevich B, Reshef R. Systemic bud induction and retinoic acid signaling underlie whole body regeneration in the urochordate *Botrylloides leachi*. PLoS Biol. 2007; 5:900–913.

Rinkevich Y, Rinkevich B, Reshef R. Cell signaling and transcription factor genes expressed during whole body regeneration in a colonial chordate. BMC Dev Biol. 2008; 8:100. [PubMed: 18847507]

Rinkevich Y, Rosner A, Rabinowitz C, Lapidot Z, Moiseeva E, Rinkevich B. Piwi positive cells that line the vasculature epithelium, underlie whole body regeneration in a basal chordate. Dev Biol. 2010; 345:94–104. [PubMed: 20553710]

Rosner A, Paz G, Rinkevich B. Divergent roles of the DEAD-box protein BS-PL10, the urochordate homologue of human DDX3 and DDX3Y proteins, in colony astogeny and ontogeny. Dev Dyn. 2006; 235:1508–1521. [PubMed: 16518819]

Rosner A, Rabinowitz C, Moiseeva E, Voskoboynik A, Rinkevich B. BS-cadherin in the colonial urochordate *Botryllus schlosseri*: one protein, many functions. Dev Biol. 2007; 304:687–700. [PubMed: 17316601]

Rosner A, Moiseeva E, Rinkevich Y, Lapidot Z, Rinkevich B. Vasa and the germ line lineage in a colonial urochordate. Dev Biol. 2009; 331:113–128. [PubMed: 19406116]

Rychel AL, Smith SE, Shimamoto HT, Swalla BJ. Evolution and development of the chordates: collagen and pharyngeal cartilage. Mol Biol Evol. 2006; 23:541–549. [PubMed: 16280542]

Stoner DS, Weissman IL. Somatic and germ cell parasitism in a colonial ascidian: possible role for a highly polymorphic allorecognition system. Proc Natl Acad Sci U S A. 1996; 93:15254–15259. [PubMed: 8986797]

Stoner DS, Rinkevich B, Weissman IL. Heritable germ and somatic cell lineage competitions in chimeric colonial protochordates. Proc Natl Acad Sci USA. 1999; 96:9148–9153. [PubMed: 10430910]

Sabbadin A, Zaniolo G, Majone F. Determination of polarity and bilateral asymmetry in palleal and vascular buds of the ascidian Botryllus schlosseri. Dev Biol. 1975; 46:79–87. [PubMed: 1158028]

Sabbadin A, Zaniolo G. Sexual differentiation and germ cell transfer in the colonial ascidian *Botryllus schlosseri*. J Exp Zool. 1979; 207:289–304.

Sunanaga T, Satoh M, Kawamura K. The role of Nanos homologue in gametogenesis and blastogenesis with special reference to male germ cell formation in the colonial ascidian, *Botryllus primigenus*. Dev Biol. 2008; 324:31–40. [PubMed: 18793630]

Thorpe A, Thorndyke MCA. The endostyle in relation to iodine binding. Symp Zool Soc Lond. 1975; 36:159–177.

Voskoboynik A, Simon-Blecher N, Soen Y, Rinkevich B, De Tomaso AW, Ishizuka KJ, Weissman IL. Striving for normality: whole body regeneration through a series of abnormal generations. FASEB J. 2007; 21:1335–1344. [PubMed: 17289924]

Voskoboynik A, Soen Y, Rinkevich Y, Rosner A, Ueno H, Reshef R, Ishizuka KJ, Palmeri KJ, Moiseeva E, Rinkevich B, Weissman IL. Identification of the endostyle as a stem cell niche in a basal chordate. Cell Stem Cell. 2008; 3:456–464. [PubMed: 18940736]

Weissman IL. Stem cells: units of development, units of regeneration, and units in evolution. Cell. 2000; 100:157–168. [PubMed: 10647940]

NIH-PA Author Manuscript

NIH-PA Author Manuscript

NIH-PA Author Manuscript

Highlights

1. Identification of a niche for germ-line and somatic stem cells in a basal chordate.
2. Stem cells repeatedly migrate between aged/damaged niches into developing niches.

NIH-PA Author Manuscript
NIH-PA Author Manuscript
NIH-PA Author Manuscript

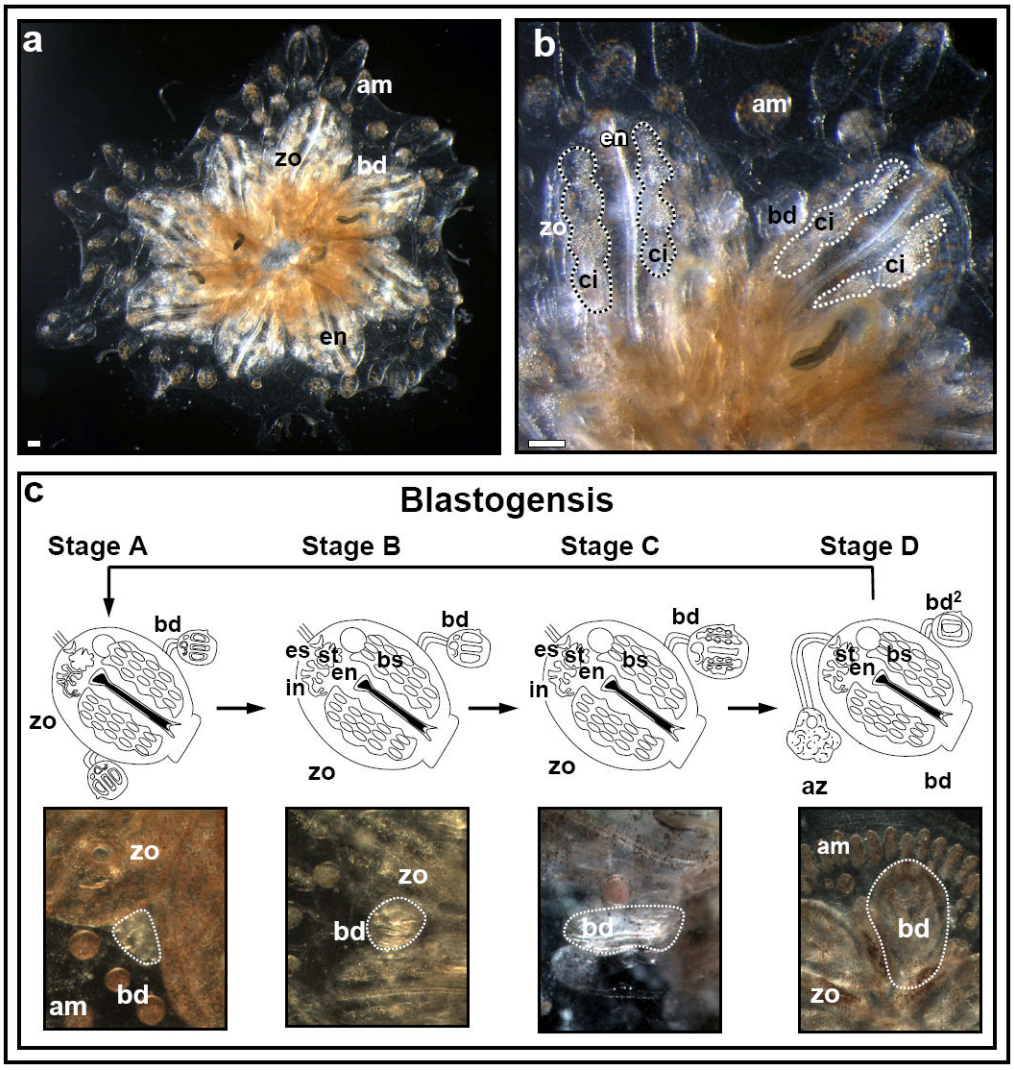

Figure 1. The anatomy and developmental cycle (blastogenesis) of *Botryllus schlosseri*

(**A**). A *Botryllus schlosseri* colony composed of a system of eight zooids (zo) and developing buds (bd), fringed at the periphery by blood-vessel termini called ampullae (am). (**B**) High power magnification of a *Botryllus schlosseri* colony. Each adult zooid houses a feeding branchial grove, termed endostyle (en), along with several lateral blood cell aggregates (termed 'cell-islands'; ci) within CI niches. (**C**) Colonies of botryllid ascidians grow through weekly cycles of development termed blastogenesis. Each blastogenic cycle is composed of four major stages (A-D), during which, new buds emerge from the body wall of each parental zooid. Each blastogenic cycle ends in a massive apoptotic and phagocytic event of all parental zooids concurrent with fast development of primary buds to the adult zooid stage (stage D, also called 'takeover'). Scale bars=100μm.

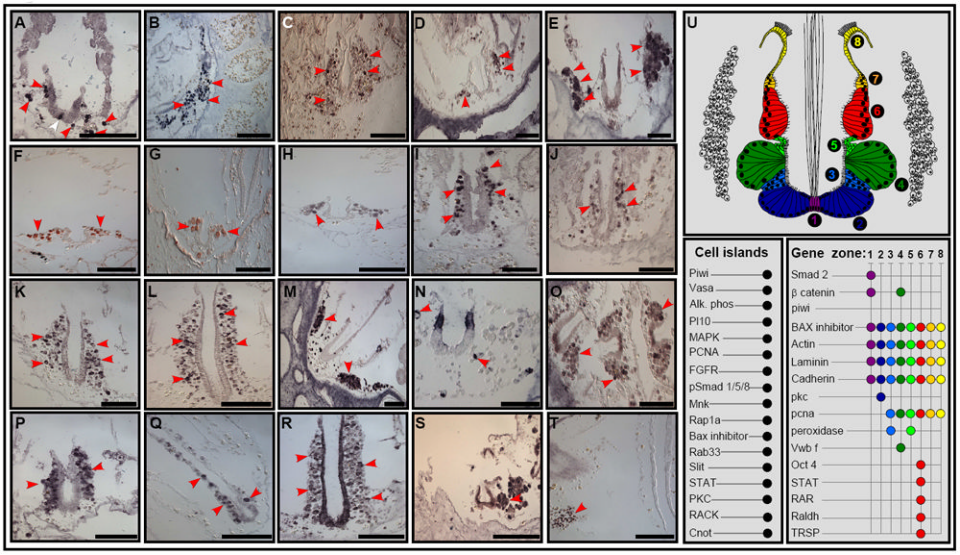

Figure 2. Molecular profile of the endostyle CIs

In-situ hybridization and immunostaining on transverse sections of the endostyle organ and CIs. *Piwi* (**A,B**, red arrows). *Alkaline-phosphatase* enzyme activity (**C**, red arrows). *Vasa* (**D**, red arrows). *Pl10* (**E**, red arrows). *PCNA* (**F**, red arrows). *FGFR* (**G**, red arrows). *MAPK* (**H**, red arrows). *Mnk* (**I**, red arrows). *Rap1A* (**J**, red arrows). *Rab33* (**K**, red arrows). *Slit* (**L**, red arrows). *pSmad 1/5/8* (**M**, red arrows). *STAT* (**N**, red arrows). *PKC* (**O**, red arrows). *RACK* (**P**, red arrows). *Cnot* (**Q**, red arrows). *Bax inhibitor* (**R**, red arrows). *Cadherin* (**S**, red arrows). *Ficolin* (**T**, red arrows). An illustration of a transverse section through the endostyle and CIs, with a summary of the expression patterns of genes (**U**). The endostyle contains eight major epithelial zones (1-8) and is bathed in large blood sinuses which harbor several pairs of compact, blood cells aggregates (termed ‘cell islands’, CIs). Scale bars: a-t=100μm. See also Figure S1.

NIH-PA Author Manuscript NIH-PA Author Manuscript NIH-PA Author Manuscript

NIH-PA Author Manuscript
NIH-PA Author Manuscript
NIH-PA Author Manuscript

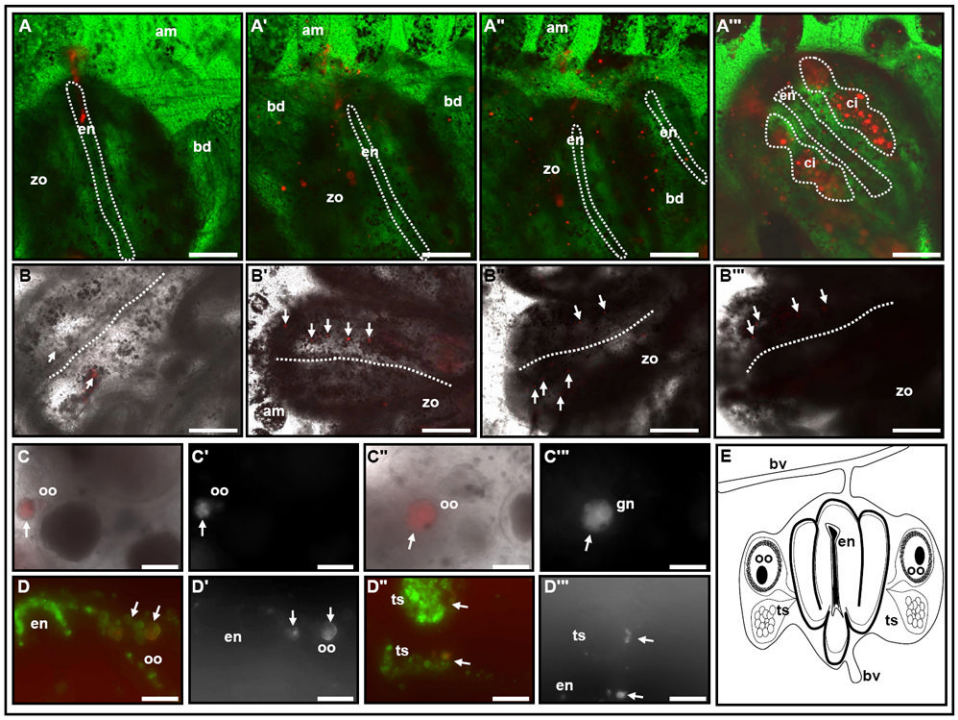

Figure 3. Putative stem cell migrations to developing CIs and the germ-line

Fate of labeled EN cells: (**A-A'"**, the endostyle is outlined by a dotted line). Representative Vybrant DiD labeling (665nm emission spectra) of 20-60 EN cells (red) of a colony at blastogenic stage B (**A**). Labeled cells proliferate within the inter-zooid sinuses and migrate to developing buds during blastogenic stage B (**A**') and throughout stage C (**A**"). Mature primary bud replacing the old generation zooid on blastogenic stage D; labeled cells are detected within the new generation of zooids sinuses and in CIs lateral to the endostyle (**A**'", red; CIs: dotted circle). Fate of labeled CI cells (**B-B**'", white arrows). Representative label of 10-50 cells from the anterior CI, within a colony at blastogenic stage B (**B**, white arrows). During blastogenic stages B,C, labeled cells appear within posterior CIs and on both lateral sides within the same zooid (**B**', **B**"; white arrows; two representative zooids 3 days following CI labeling). Following 'take-over' labeled cells reappear in newly developed CIs (**B**'", white arrows; 6 days following CI labeling). Labeled oocytes (**C-C**'", **D, D**', white arrows) and testis (**D**", **D**'", white arrows) within the gonads of a subsequent generation, 10 days following initial label. Dotted line in **B-B**'" outlines the endostyle groove. (**E**) Schematic illustration of the zooid anatomy as seen in cross sections in **C** and **D**. am, ampullae; bd, primary bud; bv, blood vessel; ci, cell island; en, endostyle; oo, oocyte; ts, testis; zo, zooid. A-C'" *in vivo* imaging; D-D'" frozen sections. Longer exposure times were used to detect and image the descendent of the EN / CI Vybrant DiD labeled cells A'-A'" and B'- C'" compare to A and B. Scale bars=100μm. See also Figure S2.

NIH-PA Author Manuscript
NIH-PA Author Manuscript
NIH-PA Author Manuscript

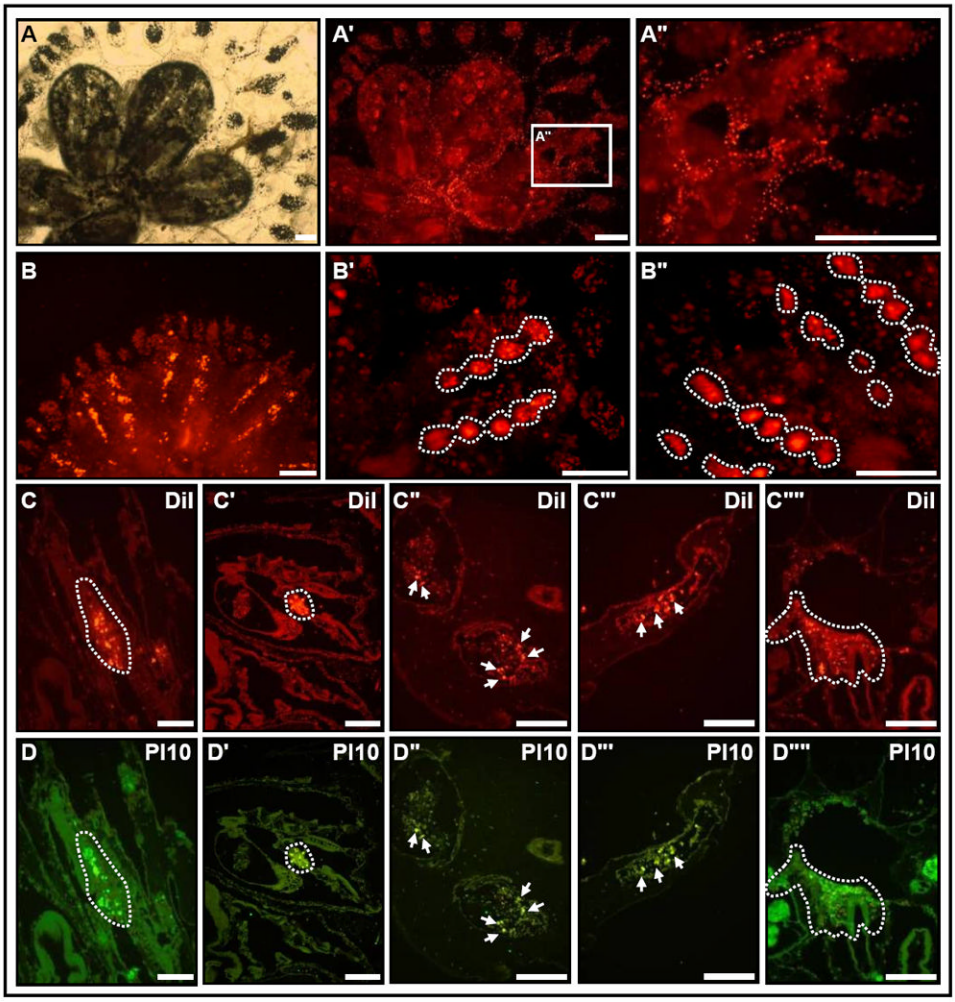

Figure 4. Repeated, long-term cycling of CI cells between niches

A colony of *Botryllus schloserri* (**A**, bright-field; **A**', fluorescence image, **A**" high power image of box in **A**') following infusion of DiI-labeled cells that were taken from EN niches and transplanted to vasculature. Allografted cells migrate within the vasculature (**A**"). Following 'take-over', labeled cells reconstitute the CIs in developed buds (**B**, 2nd blastogenic cycle). Repeated, long-term repopulations of CIs are observed following each new blastogenic cycle (**B**', **B**", 3rd and 4th blastogenic cycles, respectively). During each cycle, CI cells colonize the branchial sack (**C, C**', dotted circle), ampullae (**C**", **C**'", white arrows) and siphon (**C**"", dotted lines). Pl-10 protein co-localizes with the somatic progeny from transplanted CI cells (**D-D**""). The fluorescent DiI label is brighter compare to the colonial natural fluorescent background (501nm and 565nm emissions spectra). Scale bars=100μm. See Figure S3.

NIH-PA Author Manuscript
NIH-PA Author Manuscript
NIH-PA Author Manuscript

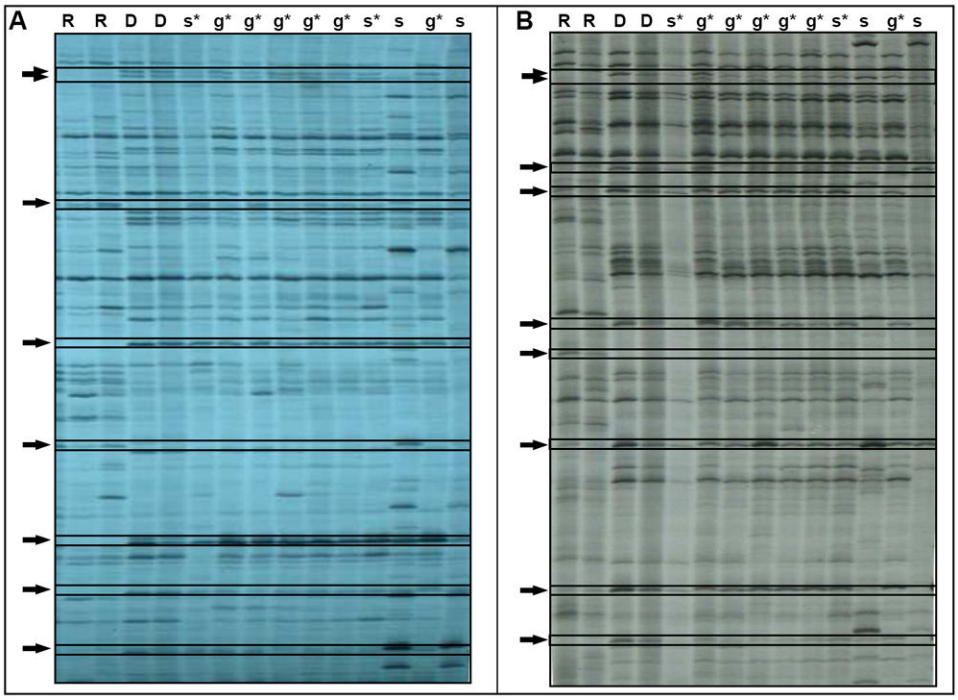

Figure 5. Transplantation of CIs induces long-term germ-line and somatic cell chimerism in recipient colonies

(**A, B**) Two representative gels showing the AFLP genetic fingerprints of naïve recipient (R) and donor (D) colonies prior to their transplantation, and genetic fingerprints of DNA samples taken from both germ-line (g) and somatic tissues (s) from recipient colonies 86 days following transplantation of cells from 3 CIs. Asterisk indicates the presence of donor fingerprints in recipient tissues (chimerism). Arrows indicate AFLP bands that differ between the recipient and the donor colonies. To ensure consistency of AFLP fingerprints and detection of chimerism, two different AFLP's primer sets were used (**A, B**), both revealed the same results. See Figure S4.

NIH-PA Author Manuscript
NIH-PA Author Manuscript
NIH-PA Author Manuscript

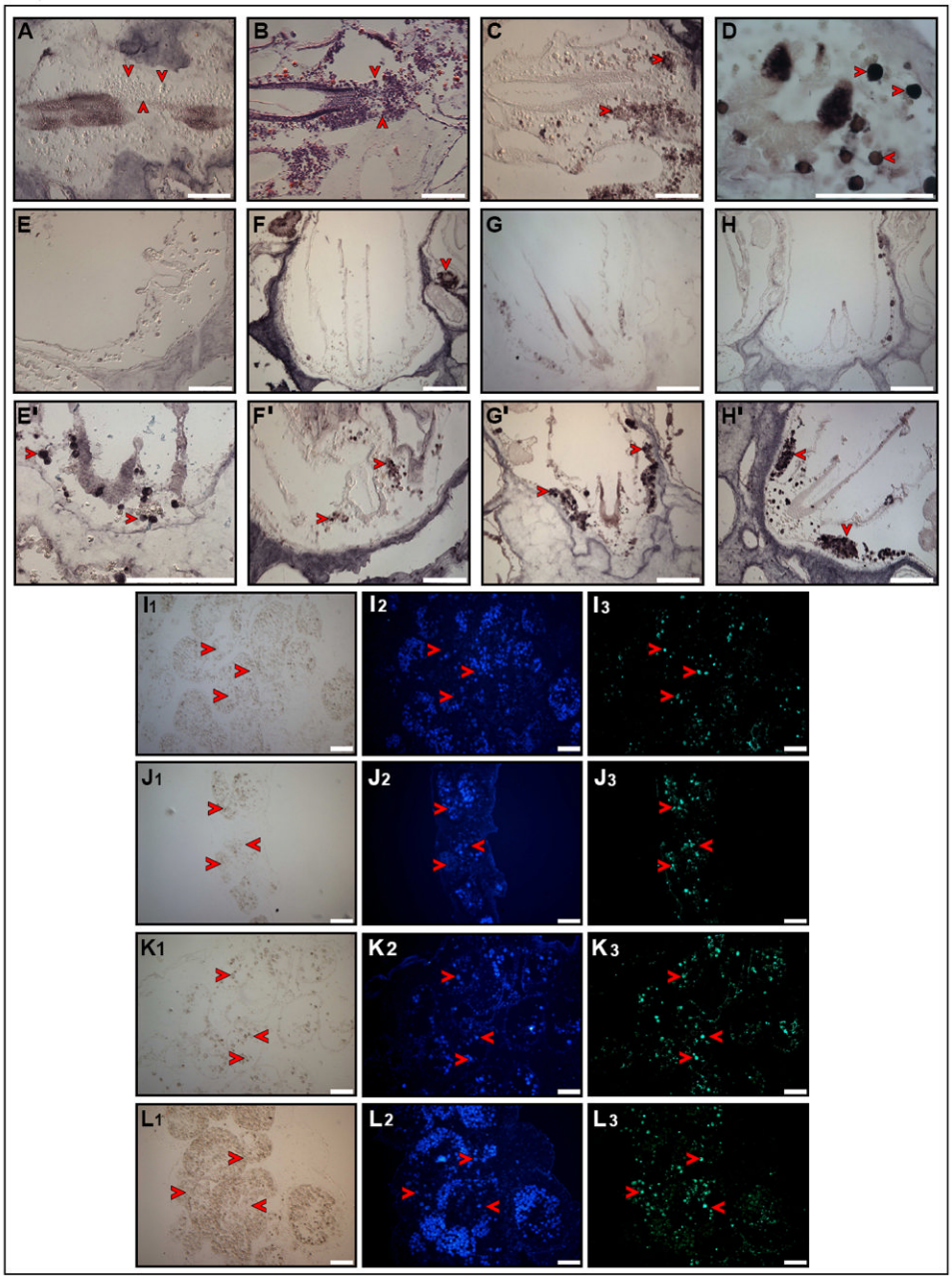

Figure 6. *Cadherin* RNAi leads to dislocation of putative stem cells from the niche

Reduction of *Cadherin* protein within EN and CIs of *Cadherin* RNAi treated colonies (**A**, arrowheads). Hematoxylin and eosin staining showing scattered cells resulting from disorganized morphology of EN and CI (**B**, arrowheads). *PCNA* protein is expressed within scattered CI cells (**C**, arrowheads). *Oct4* protein is expressed within scattered EN cells (**D**, arrowheads). Putative stem cells are lost from CIs of *Cadherin* RNAi treated colonies (**E-H**) compare to control colonies (**E'-H'**). *Piwi* protein (**E, E'**, arrowheads). *Vasa* protein (**F, F'**, arrowheads). *Pl10* (**G, G'**, arrowheads). *pSmad1/5/8* protein (**H, H'**, arrowheads). Putative stem cells reappear in the circulation of *Cadherin* RNAi treated colonies. *Piwi* protein (**I1-I3**, arrowheads). *Vasa* protein (**J1-J3**, arrowheads). *Pl10* protein (**K1-K3**, arrowheads). *PCNA* protein (**L1-L3**, arrowheads). Scale bars=100μm. See Figure S5.

NIH-PA Author Manuscript

NIH-PA Author Manuscript

NIH-PA Author Manuscript

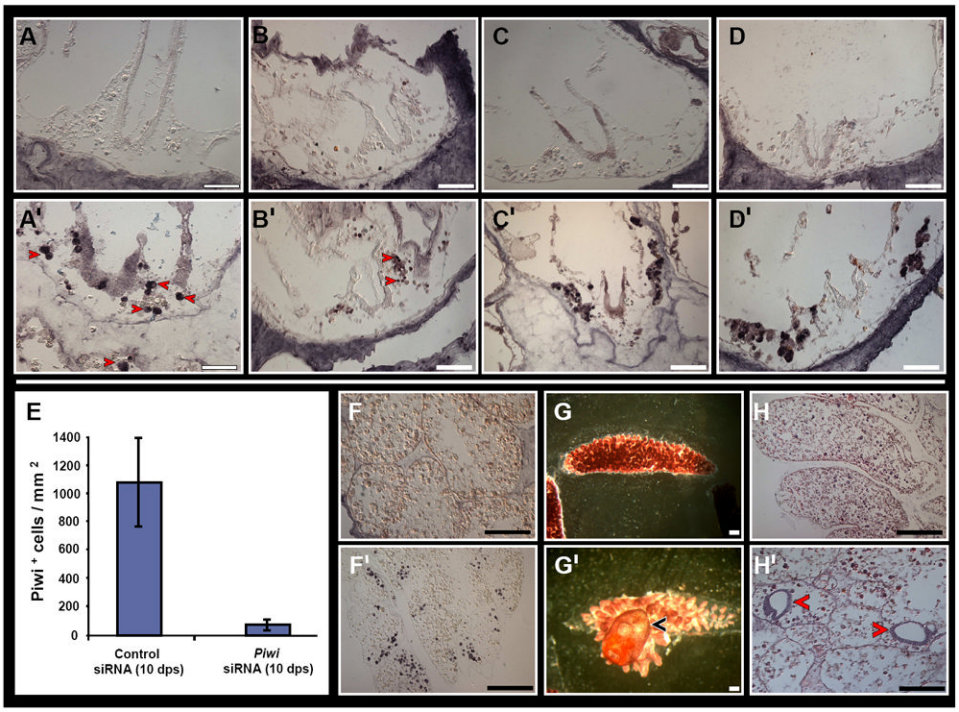

Figure 7. *Piwi* RNAi in *B. leachi* colonies leads to depletion of stem cells markers within CIs and the colony circulation and regeneration arrest

CIs of RNAi treated (A-D) and control colonies (**A'-D'**). *Piwi* protein (**A, A'**). *Vasa* protein (**B, B'**). *Pl10* ptotein (**C, C'**). *PCNA* protein (**D, D'**). Diagram depicting a decline in *Piwi*$^+$ cells within the circulation of RNAi treated fragments (**E**). RNAi treated (**F-H**) and control (**F'-H'**) regenerating fragments at 16 days post separation. *Piwi*$^+$ cells are absent from RNAi treated fragments (**F**) compared to same-stage regenerating controls which show a systemic distribution of *Piwi*$^+$ cells within multiple sites (**F'**). A 16 day RNAi treated fragment displaying a blood-vessel lacunae with absence of a regenerating zooid (**G**). A same stage regenerating control fragment displaying a regenerated zooid with incurrent and outcurrent siphons (**G'**, arrowhead). Hematoxylin and eosin staining shows absence of developing buds in RNAi treated fragments (**H**) and two developing buds in same-stage controls (**H'**, arrowheads). Scale bars=100μm. See Figure S6.